

## Electronic Supporting Information

### **A Robust Binary Supramolecular Organic Framework (SOF) with High CO<sub>2</sub> Adsorption and Selectivity**

Jian Lü,<sup>a,b</sup> Cristina Perez-Krap,<sup>a</sup> Mikhail Suyetin,<sup>a</sup> Nada Al Smail,<sup>a</sup> Yong Yan,<sup>a</sup> Sihai Yang,<sup>a</sup> William Lewis,<sup>a</sup> Elena Bichoutskaia,<sup>a</sup> Chiu C. Tang,<sup>c</sup> Alexander J. Blake,<sup>a</sup> Rong Cao<sup>b</sup> and Martin Schröder<sup>\*a</sup>

*<sup>a</sup>School of Chemistry, University of Nottingham, University Park, Nottingham NG7 2RD, UK. Fax: +44 115 951 3563; E-mail: M.Schroder@nottingham.ac.uk*

*<sup>b</sup>State Key Laboratory of Structural Chemistry, Fujian Institute of Research on the Structure of Matter, Chinese Academy of Sciences, Fujian, Fuzhou 350002, P. R. China*

*<sup>c</sup>Diamond Light Source, Harwell Science and Innovation Campus, Didcot, OX11 0DE, UK.*

*\*Corresponding author.*

## Chemicals and General methods

Commercially available reagents and organic solvents were used as received without further purification. Elemental analyses (C, H, and N) were performed on a CE-440 elemental analyzer. Infrared (IR) spectra were recorded with a PerkinElmer Spectrum One with KBr pellets in the range 400–4000  $\text{cm}^{-1}$ , or on a Nicolet iS5 FT-IR spectrophotometer in the range of 550–4000  $\text{cm}^{-1}$  using the attenuated total reflectance (ATR) mode.  $^1\text{H}$  NMR spectra were recorded on a Bruker DPX-400 spectrometer. Thermal gravimetric analyses (TGA) were performed under a flow of nitrogen (20  $\text{mL}\cdot\text{min}^{-1}$ ) with a heating rate of 10  $^\circ\text{C}\cdot\text{min}^{-1}$  using a TA SDT-600 thermogravimetric analyzer. X-ray powder diffraction (PXRD) measurements were carried out at room temperature on a PANalytical X'Pert PRO diffractometer using Cu-K $\alpha$  radiation ( $\lambda = 1.5418 \text{ \AA}$ ) at 40 kV, 40 mA, at a scan speed of 0.02 $^\circ$ /s and a step size of 0.005 $^\circ$  in  $2\theta$ .  $\text{N}_2$ ,  $\text{H}_2$ ,  $\text{CO}_2$  and  $\text{CH}_4$  isotherms were recorded using an IGA gravimetric adsorption apparatus (Hiden) at the University of Nottingham in a clean ultra-high vacuum system with a diaphragm and turbo pumping system. Before measurement, about 60 mg solvent-exchanged sample was loaded into the sample basket within the adsorption instrument and then degassed under dynamic vacuum at 100  $^\circ\text{C}$  for 24 hours to obtain the fully desolvated sample.

## Experimental

**Synthesis of 3-Amino-3-(4-pyridinyl)-propionitrile<sup>S1</sup>:** 4-Cyanopyridine (104 mg, 1.0 mmol), in MeCN (82 mg, 2.0 mmol), and potassium *tert*-butoxide (336 mg, 3.0 mmol) were added to toluene (40 mL) and the reaction mixture stirred at ambient temperature for 48 h. Saturated  $\text{NaHCO}_3$  solution (200 mL) was used to quench the reaction, and the resultant solid crude product of 3-amino-3-(4-pyridinyl)-propionitrile was collected by filtrations and washed three times with NaCl solution and dried in air. Yield: 76%.  $^1\text{H}$  NMR ( $\text{DMSO}-d_6$ ): 8.63 (d,  $J = 6.3 \text{ Hz}$ , 2H, 2,6-Pyridyl-H); 7.57 (d,  $J = 6.0 \text{ Hz}$ , 2H, 3,5-Pyridyl-H); 7.01 (s, 2H, NH), 4.4 (s, 1H, =C-H) ppm. HRMS (EI-):  $m/z$  439.0403 [ $M+\text{H}$ ] $^+$ . IR (KBr,  $\nu_{\text{max}}$ ,  $\text{cm}^{-1}$ ): 2801 (w), 2759 (w), 2256 (m), 2194 (s), 1942 (m), 1670 (s), 1593 (s),

1530 (s), 1502 (s), 1425 (s), 1335 (m), 1271 (m), 1222 (m), 1146 (m), 1069 (m), 992 (s), 874 (m), 839 (s), 670 (s), 650 (s), 609 (s), 573 (s). Elemental analysis for C<sub>8</sub>H<sub>7</sub>N<sub>3</sub> (found/calcd): C, 66.15/66.19; H, 4.83/4.86; N, 28.94/28.95.

**Synthesis of 1,4-bis-(4-(3,5-dicyano-2,6-dipyridyl)dihydropyridyl)benzene<sup>S1a</sup> (1):** 3-Amino-3-(4-pyridinyl)-propionitrile (580 mg, 4.0 mmol) and 1,3-benzenedialdehyde (134 mg, 1.0 mmol) were added to acetic acid (10 mL) under N<sub>2</sub> and the reaction mixture refluxed at 120 °C for 48 h. The light yellow precipitate of **1** was collected by filtration and washed with hot acetic acid, EtOH, and distilled water and dried in air. Yield: 61% <sup>1</sup>H NMR (DMSO-*d*<sup>6</sup>): 10.4 (s, 2H, dihydropyridyl-NH), 8.7 (d, *J* = 4.7 Hz, 8H, Py-H), 7.7 (d, *J* = 4.7 Hz, 8H, Py-H); 7.65 (s, 4H, Ar-H), 4.9 (s, 2H, dihydropyridyl-CH) ppm. HRMS (EI-): *m/z* 643.21 [*M*+H]<sup>+</sup>. IR (KBr, ν<sub>max</sub>, cm<sup>-1</sup>): 2205 (s), 1756 (w), 1718 (m), 1645 (m), 1599 (s), 1550 (m), 1516 (s), 1417 (m), 1345 (m), 1295 (s), 1273 (m), 1246 (w), 1215 (m), 1189 (w), 1155 (w), 1071 (w), 999 (w), 831 (m), 801 (w), 744 (w), 694 (w), 668 (w), 653 (w), 591 (m), 521 (w). Elemental analysis for C<sub>40</sub>H<sub>24</sub>N<sub>10</sub> (found/calcd): C, 74.80/74.52; H, 3.96/3.75; N, 21.22/21.73.

This reaction is very similar to that previously reported for the synthesis of **3**.<sup>S1b</sup> We were however unable to prepare significant amounts of **3** directly by this published route, and in our hands the synthesis of **1** was more reliable and generated the desired products.

**Synthesis of 5,5'-Bis-(azanediyl)-oxalyl-diisophthalic acid<sup>S2</sup> (2):** A solution of 5-aminoisophthalic acid (6.53g, 34.2mmol) in anhydrous THF (50 mL) was cooled at 0 °C. A solution of oxalyl chloride (1.0 mL, 11.4 mmol) in anhydrous THF (100mL) was added dropwise to the above solution over 1 h, during which a precipitate formed almost immediately. Triethylamine (1.0 mL, 7.2 mmol) was slowly added after 1 h and the mixture was stirred overnight at room temperature. 2M HCl (200 mL) was then added and the white precipitate of **2** was filtered and washed with water, and recrystallized

from MeOH. The product was further washed with MeOH and diethyl ether and dried under vacuum to afford a white powder. Yield: 58%.  $^1\text{H NMR}$  ( $\text{DMSO-}d^6$ ): 13.08 (s, 4H, COOH); 11.26 (s, 2H, NH); 8.72 (d,  $J = 1.2$  Hz, 4H, Ar-H); 8.26 (t,  $J = 1.2$  Hz, 2H, Ar-H). ATR FT-IR ( $\nu_{\text{max}}$ ,  $\text{cm}^{-1}$ ): 2158 (w), 1974 (w), 1716(s), 1681(s), 1653(s), 1558 (m), 1540 (s), 1456 (m), 1387 (s), 1301(m), 1275 (s), 1185 (w), 952 (m), 841(m), 758 (s), 728 (s), 670 (m). HRMS (EI-):  $m/z$  439.0403 [ $M+\text{Na}$ ] $^+$ , 434.0838 [ $M+\text{H}_4\text{N}$ ] $^+$ , 415.0401 [ $M-\text{H}$ ] $^-$ . Elemental analysis for  $\text{C}_{18}\text{H}_{12}\text{N}_2\text{O}_{10}$  (found/calcd): C, 51.93/51.47; H, 2.90/3.05; N, 6.73/6.56.

**Synthesis of  $[(\text{C}_{18}\text{H}_{12}\text{N}_2\text{O}_{10})\cdot(\text{C}_{40}\text{H}_{20}\text{N}_{10})]\cdot 7\text{DMF}$  (SO $\text{F-7}$ ):** 1,4-Bis-(4-(3,5-dicyano-2,6-dipyridyl)dihydropyridyl)benzene (**1**) (33 mg, 0.05 mmol) and 5,5'-bis-(azanediyl)-oxalyl-diisophthalic acid (**2**) (21 mg, 0.05 mmol) were added to DMF (3mL). The reaction mixture was transferred into a 15 mL pressure tube and heated in oil bath at 90 °C and autogenous pressure for 3 days. Orange crystals were collected by filtration and washed with cold DMF to give pure phase of **SO $\text{F-7}$** . Yields: *ca.* 58%. IR (KBr,  $\nu_{\text{max}}$ ,  $\text{cm}^{-1}$ ): 2459 (w), 2359 (w), 2231 (w) 1712 (s), 1662 (s), 1598 (m), 1558 (w), 1530 (m), 1392 (m), 1251 (s), 1101(m), 1060 (m), 1051 (m), 841(m), 800 (w), 764 (m), 686 (w), 659 (w), 609 (w), 572 (w), 499 (w). Elemental analysis for  $\text{C}_{79}\text{H}_{81}\text{N}_{19}\text{O}_{17}$  (**SO $\text{F-7}$** , found/calcd): C, 60.49/61.31; H, 5.20/4.48; N, 16.97/16.61; for  $\text{C}_{58}\text{H}_{32}\text{N}_{12}\text{O}_{10}$  (**SO $\text{F-7a}$** , found/calcd): C, 65.86/63.97; H, 3.05/3.18; N, 15.89/15.63.

**Sample activation:** As-prepared **SO $\text{F-7}$**  was exchanged with acetone, and degassed under dynamic vacuum at 100 °C for 24 hours to afford the activated desolvated sample **SO $\text{F-7a}$** . **SO $\text{F-7a}$**  retains its crystallinity and framework integrity as confirmed by PXRD (Figure S2). Moreover, the desolvated sample **SO $\text{F-7a}$**  exhibits excellent durability towards both common organic solvents and water, even in boiling water (Figure S3). Recovery of **SO $\text{F-7a}$**  sample as a crystalline material after gas adsorption experiments was realized by soaking the material in acetone or ethanol followed by the above activation (Figure S3).

## Crystallography

Single crystal X-ray data was collected on Agilent GV1000 X-ray diffractometer at the University of Nottingham. Details of the data collection are included in the CIF. The structure was solved by direct methods and developed by difference Fourier techniques, both using the SHELXL software package.<sup>S3</sup> The hydrogen atoms of the ligands were placed geometrically and refined using a riding model. The unit cell volume includes a large region of disordered solvent which could not be modeled as discrete atomic sites. We therefore employed PLATON/SQUEEZE<sup>S4</sup> to calculate the contribution of the solvent region to the diffraction and thereby produced a set of solvent-free diffraction intensities.

## Heats of Adsorption

The heats of adsorption ( $Q_{st}$ ) were calculated using the Clausius Clapeyron equation (1) for CO<sub>2</sub> for isotherms at 273K and 293K and were solved by a virial-type equation (2).

$$\frac{d \ln(p)}{d(1/T)} = -\frac{\Delta H}{R} \quad (1)$$

Where  $p$  is pressure,  $T$  is the temperature,  $R$  is the real gas constant;

$$\ln(n/p) = A_0 + A_1 n + A_2 n^2 + \dots \quad (2)$$

Where  $p$  is the pressure,  $n$  is the amount adsorbed,  $A_i$  is *Virial* coefficients, and  $i$  represents the number of coefficients required to adequately describe the isotherms with low uptakes.

*Tóth method* (Table S4)

The non-linear equation (3) was used

$$n = n_{\text{sat}} \left( b^{1/t} / 1 + b^t \right)^{1/t} \quad (3)$$

where  $n$  is the uptake in mmol·g<sup>-1</sup>,  $n_{\text{sat}}$  is the saturation uptake mmol·g<sup>-1</sup>,  $t$  and  $b$  are parameters which are specific for adsorbate-adsorbant pairs. The value of parameter  $t$  is usually less than unity

and is said to characterize the system heterogeneity. The Henry's law constant  $K_H$ , quantifies the extent of the adsorption of a given adsorbate by a solid. For the Tóth isotherm, the Henry's law constant is defined by the following equation (4):

$$K_H \lim_{p \rightarrow 0} \left( \frac{dn}{dp} \right) = b^{1/\tau} n_{\text{sat}} \quad (4)$$

#### *Dubinin Asthakov Method*

In order to determine the pore size distribution, the CO<sub>2</sub> adsorption isotherm at 273K was fitted using the *Dubinin Asthakov* (D.A) model (Eq. 5).

$$n_{\text{ad}} = n_p \exp \left( -\frac{RT}{E_0} \ln \left[ \frac{P_0}{P} \right] \right)^n \quad (5)$$

where  $n_{\text{ad}}$  is the experimental adsorption,  $n_p$  is the microporous limit capacity and  $E_0$  is the adsorption characteristic energy based on pore filling mechanism. Equation fits calculated data to experimental isotherm by varying two parameters,  $E_0$  and  $n$ .  $E_0$  is average adsorption energy that is directly related to average pore diameter, and  $n$  is an exponent that controls the width of the resulting pore size distribution.

	$E_0$	$n$	Surface Area	Pore Volume
<b>SOF-7a</b>	8.84 kJ·mol <sup>-1</sup>	2.7	913 m <sup>2</sup> ·g <sup>-1</sup>	0.32 cm <sup>3</sup> ·g <sup>-1</sup>

#### **Grand Canonical Monte Carlo (GCMC) simulations**

Grand Canonical Monte Carlo (GCMC) simulations were performed to analyse the adsorption of CO<sub>2</sub> in **SOF-7a**. The simulation parameters for CO<sub>2</sub> were taken from the TraPPE force field.<sup>S5</sup> The CO<sub>2</sub> molecule was assumed to have the C–O bond length of 1.16 Å, and three charged Lennard-Jones interaction sites with the following parameters:  $\sigma_O = 3.05$  Å,  $\epsilon_O/k_B = 79$  K for oxygen atom, and  $\sigma_C = 2.80$  Å and  $\epsilon_C/k_B = 27$  K for carbon atom. A point charge of +0.7 was placed at the centre of mass of carbon atom and a point charge of –0.35 was placed at oxygen atom. Atomic parameters for the framework structure were described by the OPLS-AA force

field<sup>S6</sup> and for oxygen atoms present in **SOF-7a**, the modelling atomic parameters were taken from and adjusted for a correct description of the interaction between guest CO<sub>2</sub> molecules and the host SOF.<sup>S7</sup> The supercell used to represent **SOF-7a** in simulations contained 5 (5x1x1) unit cells, and periodic boundary conditions were applied to the supercell. The fugacity was calculated from the Peng-Robinson equation of state,<sup>S8</sup> and the Lennard-Jones (LJ) potential used to describe the Van der Waals interactions with a cut-off distance of 12.8 Å. The partial charges on atoms of the **SOF-7a** were computed using the CHELPG approach and the B3LYP/6-31G\* level of density functional theory (DFT), as implemented in Q-Chem quantum chemistry package.<sup>S9</sup> The GCMC simulations were performed with *MUSIC* simulation suite<sup>S10</sup> and included 2·10<sup>7</sup> step equilibration period followed by 2·10<sup>7</sup> step production run.

### **Binding energy calculations**

Density functional calculations (DFT), as implemented in the Q-Chem quantum chemistry package, was employed to analyze in detail the strength of the preferred adsorption sites in **SOF-7a**, calculate the binding energies (BE) between CO<sub>2</sub> molecule and the framework, and reveal and describe configurations corresponding to the strongest binding. The calculations were performed in two-stages: the geometry optimization was carried out at the B3LYP/6-31G\*\* level of theory with dispersion correction taken into account,<sup>S11</sup> and the binding energies were subsequently calculated at the higher B3LYP/6-311++G\*\* level with dispersion correction as follows:

$$\mathbf{BE} = \mathbf{E}(\mathbf{complex}) - \mathbf{E}(\mathbf{linker}) - \mathbf{E}_{\mathbf{opt}}(\mathbf{CO}_2)$$

The BE was corrected for basis set superposition error (BSSE). Several energy minimum configurations revealed strong binding, and their properties are summarized in the Table S4.

**Table S1** Crystallographic data for **SOF-7**

Compounds	<b>SOF-7</b>
Chemical formula	$C_{79}H_{81}N_{19}O_{17}$
Formula mass	1568.62
Crystal system	Monoclinic
Space group	$C2/c$
$a/\text{\AA}$	7.65676(19)
$b/\text{\AA}$	30.1426(8)
$c/\text{\AA}$	34.5158(8)
$\alpha/^\circ$	90.00
$\beta/^\circ$	93.900(2)
$\gamma/^\circ$	90.00
Cell volume/ $\text{\AA}^3$	7947.6(3)
$Z$	4
Reflections collected	46769
Independent reflections	8040
$R_{int}$	0.0354
Final $R_I$ values ( $I > 2\sigma(I)$ )	0.0456
Final $wR(F^2)$ values ( $I > 2\sigma(I)$ )	0.1367
Goodness of fit on $F^2$	1.046



**Table S2** Gas sorption data for some best performing porous supramolecular organic framework materials.

	$S_{\text{ABET}}$ ( $\text{m}^2\cdot\text{g}^{-1}$ )	$V(\text{N}_2)$ ( $\text{mmol}\cdot\text{g}^{-1}$ )		$V(\text{CH}_4)$ ( $\text{mmol}\cdot\text{g}^{-1}$ )				$V(\text{CO}_2)$ ( $\text{mmol}\cdot\text{g}^{-1}$ )			
		77 K	77 K	273 K	298 K	273 K	298 K	273 K	298 K	273 K	298 K
		1 bar	1 bar	1 bar	1 bar	20 bar	20 bar	1 bar	1 bar	20 bar	20 bar
<b>SOF-7a</b>	900 <sup>[a]</sup>	2.9	0.03	0.29	0.22	2.11	1.71	2.85	1.49	7.07	5.48
<b>HOF-8d</b> <sup>S12</sup>	--	--	--	--	--	--	--	--	2.55	--	--
<b>TTBI</b> <sup>S13</sup>	2796 <sup>[b]</sup>	34	10.8	0.94	--	--	--	3.61	--	--	--
<b>SOF-1a</b> <sup>S1</sup>	474 <sup>[c]</sup>	6.4	--	--	--	1.43 <sup>[e]</sup>	--	1.34	0.71	4.06 <sup>[e]</sup>	3.08 <sup>[e]</sup>
<b>HOF-1a</b> <sup>S14</sup>	359 <sup>[d]</sup>	--	--	--	--	--	--	--	--	--	--
<b>HOF-2a</b> <sup>S15</sup>	238 <sup>[d]</sup>	--	--	--	--	--	--	--	--	--	--
<b>TBC[4]DHQ</b> <sup>S16</sup>	230 <sup>[b]</sup>	4.0	--	--	--	--	--	--	--	--	1.56 <sup>[f]</sup>
<b>TTP</b> <sup>S17</sup>	--	--	--	--	0.38	--	--	--	0.98	--	--
<b>CB[6]</b> <sup>S18</sup>	210	--	--	--	--	--	--	2.7(8)	2.2	--	3.4 <sup>[g]</sup>
<b>CB[7]</b> <sup>S19</sup>	293 <sup>[d]</sup>	--	--	--	0.27 <sup>[h]</sup>	--	--	2.8(7)	2.3 <sup>[h]</sup>	--	--

[a] Calculated from CO<sub>2</sub> isotherm at 273 K; [b] determined by N<sub>2</sub> sorption at 77 K with data points in the range for P/P<sub>0</sub> between 0.01 and 0.04; [c] Calculated from N<sub>2</sub> adsorption at 125 K and 1 bar; [d] determined by CO<sub>2</sub> adsorption at 196 K; [e] measured at 16 bar; [f] measured at 35 bar; [g] measured at 30 bar; [h] measured at 297 K.

**Table S3** Comparison of gas uptake of **SOF-7a** and **SOF-1a** for selectivity CO<sub>2</sub> over CH<sub>4</sub> at 16 bar.

Material	CH <sub>4</sub> uptake at 1bar (mmol·g <sup>-1</sup> )		CH <sub>4</sub> uptake at 16 bar (mmol·g <sup>-1</sup> )		CH <sub>4</sub> uptake at 20 bar (mmol·g <sup>-1</sup> )		CO <sub>2</sub> uptake at 16 bar (mmol·g <sup>-1</sup> )	Selectivity CO <sub>2</sub> over CH <sub>4</sub>	
	273 K	298 K	273 K	298 K	273 K	298 K	298 K	273 K	298 K
<b>SOF-7a</b>	0.29	0.22		1.54	2.11	1.71	5.30	14.2	9.31
<b>SOF-1a</b>				1.43			3.08	5.60	4.24

**Table S4** Summary of the binding energy and parameters for CO<sub>2</sub> binding in **SOF-7a**.

<i>Dimer</i> ...CO <sub>2</sub>	<i>Binding Energy with dispersion correction (kJ·mol<sup>-1</sup>)</i>	<i>Binding Energy (kJ·mol<sup>-1</sup>)</i>	<i>Interaction</i>	<i>Distance (Å)</i>	<i>Angle (°)</i>	<i>O=C=O Angle (°)</i>	<i>Charge Transfer (me)</i>
<b>A</b>	-35.19	-10.24	H-Bond N-H...O <sub>1</sub> @CO <sub>2</sub>	2.29 H...O <sub>1</sub> @CO <sub>2</sub>	165.22 N-H...O@ CO <sub>2</sub>	178.17	+54.36
			Weak H-Bond C-H...O <sub>1</sub> @CO <sub>2</sub>	2.80 H...O <sub>1</sub> @CO <sub>2</sub>	140.59 C- H...O <sub>1</sub> @CO <sub>2</sub>		
			Weak H-Bond C-H...O <sub>2</sub> @CO <sub>2</sub>	2.79 H...O <sub>2</sub> @CO <sub>2</sub>	144.30 C- H...O <sub>2</sub> @CO <sub>2</sub>		
			CO...C@CO <sub>2</sub>	2.83 O...C@CO <sub>2</sub>	148.62 C-O...C@CO <sub>2</sub>		
<b>B</b>	-29.75	-7.96	H-Bond N-H...O@CO <sub>2</sub>	2.35 NH...O@CO <sub>2</sub>	160.76 N-H...O@ CO <sub>2</sub>	178.30	+22.72
			Weak H-Bond C-H...O@CO <sub>2</sub>	2.79 H...O@CO <sub>2</sub>	161.53 C-H...O@ CO <sub>2</sub>		
			C-O...C@CO <sub>2</sub>	2.79 O...C@CO <sub>2</sub>	147.07 C-O... C@CO <sub>2</sub>		
<b>C</b>	-31.53	-10.90	H-Bond N <sub>3</sub> -H...O@CO <sub>2</sub>	2.30 H...O@CO <sub>2</sub>	N <sub>3</sub> - H...O@CO <sub>2</sub> 152.12	178.83	-46.99
			C-N <sub>1</sub> ...C@CO <sub>2</sub>	3.00 N <sub>1</sub> ...C@CO <sub>2</sub>	148.45 C-N <sub>1</sub> ...C@CO <sub>2</sub>		
			C-N <sub>2</sub> ...C@CO <sub>2</sub>	3.00 N <sub>2</sub> ...C@CO <sub>2</sub>	138.24 C-N <sub>2</sub> ...C@CO <sub>2</sub>		
<b>D</b>	-18.87	-3.28	Weak H-Bond C-H...O <sub>1</sub> @CO <sub>2</sub>	2.68 H...O <sub>1</sub> @CO <sub>2</sub>	151.83 C- H...O <sub>1</sub> @CO <sub>2</sub>	177.60	+27.65
			Weak H-Bond C-H...O <sub>2</sub> @CO <sub>2</sub>	2.83 H...O <sub>2</sub> @CO <sub>2</sub>	154.91 C- H...O <sub>2</sub> @CO <sub>2</sub>		
			C-O...C@CO <sub>2</sub>	2.73 O...C@CO <sub>2</sub>	168.63 C-O...C@CO <sub>2</sub>		

**Table S5** Tóth fitting parameters and Henry law constants for gas uptake in **SO<sub>F</sub>-7a**

Temperature	CH <sub>4</sub>					CO <sub>2</sub>				
	n <sub>sat</sub>	b	t	R <sup>2</sup>	K <sub>H</sub>	n <sub>sat</sub>	b	t	R <sup>2</sup>	K <sub>H</sub>
273K	3.573	0.089	0.979	0.9997	0.305	8.049	0.545	0.974	0.9993	4.317
298K	1.365	0.078	1.329	0.9998	0.201	8.247	0.256	0.907	0.9996	1.836

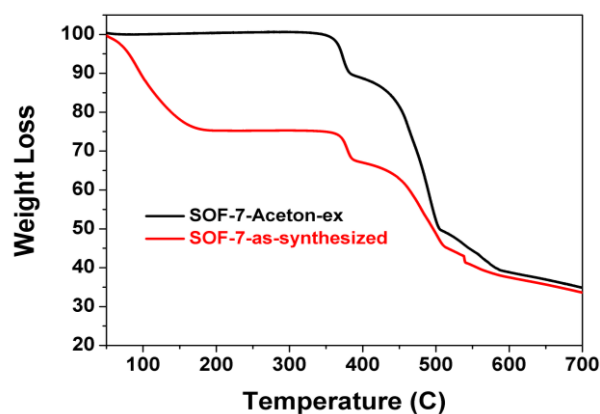


**Figure S1** Thermogravimetric analysis (TGA) of the as-synthesized and acetone-exchanged samples of **SO<sub>F</sub>-7**. Samples were dried under N<sub>2</sub> flow upon loading before recording the TGA.

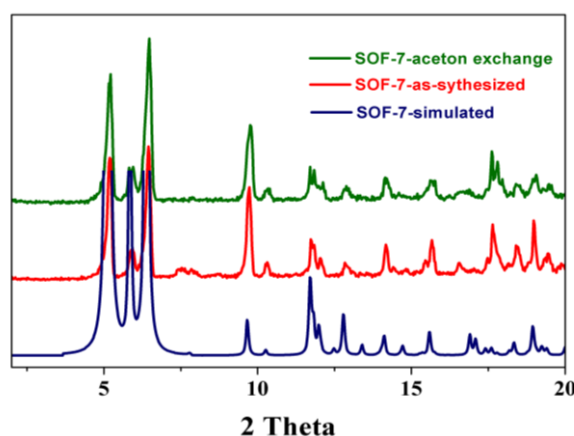


**Figure S2** Powder X-ray diffraction (PXRD) of the simulated, as-synthesized and acetone-exchanged samples of **SO<sub>F</sub>-7**.

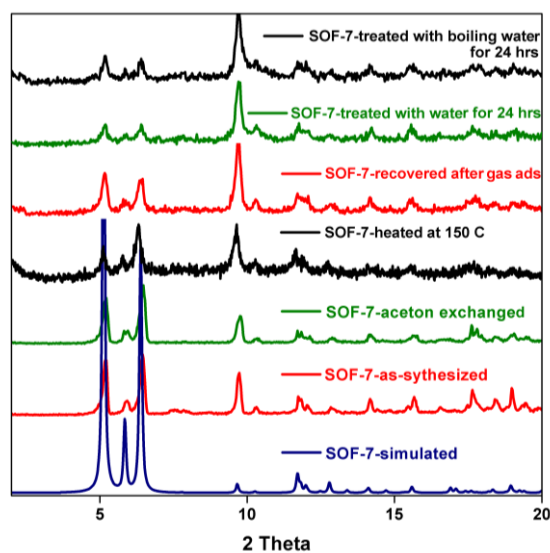


**Figure S3** PXRD data for **SOF-7** under various conditions.

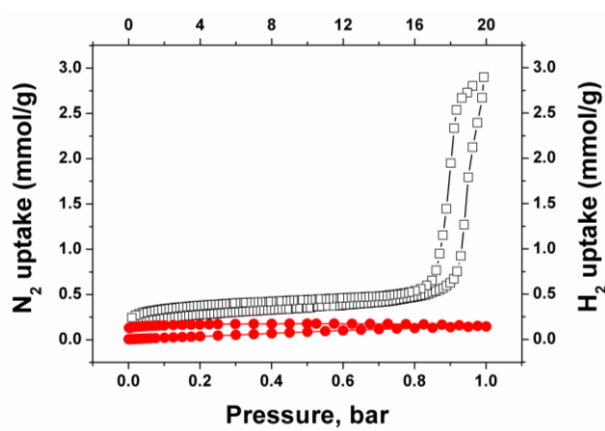


**Figure S4**  $N_2$  (black) and  $H_2$  (red) uptake isotherms for **SOF-7a** at 77 K (black) in the pressure range 0 to 1bar (for  $N_2$ ) and 0 to 20 bar (for  $H_2$ ).

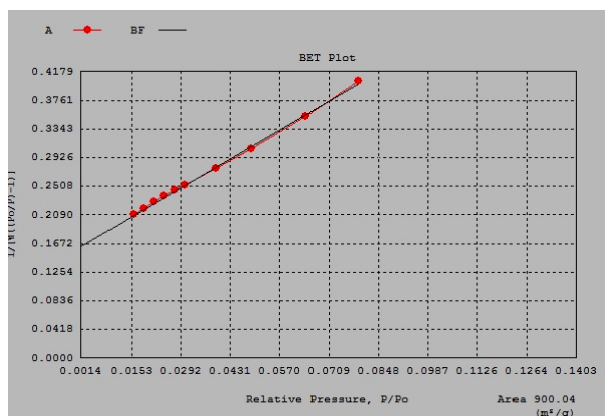


**Figure S5** Brunauer-Emmett-Teller (BET) surface area of **SOF-7a** calculated from the CO<sub>2</sub> isotherm recorded at 273 K.

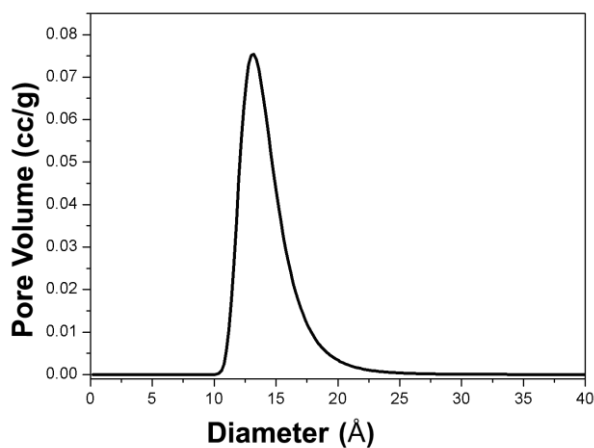


**Figure S6** Pore size distribution (PSD) plot for **SOF-7a** calculated from the CO<sub>2</sub> adsorption isotherm at 273 K using Dubinin Asthakov (DA) methods.

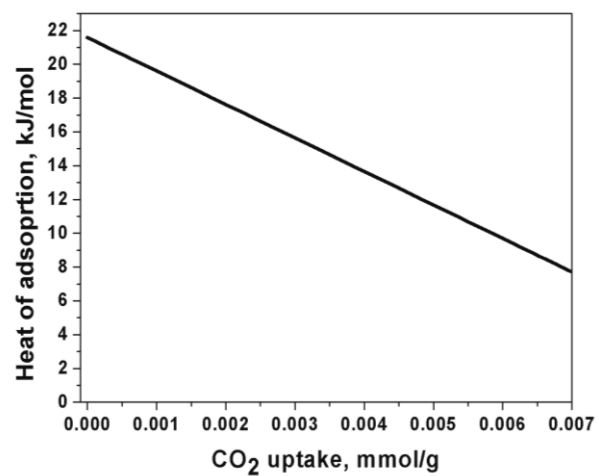


**Figure S7** Heat of adsorption for **SOF-7a**.

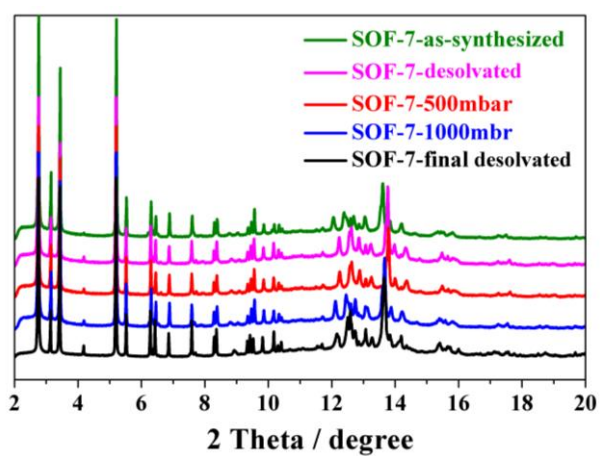


**Figure S8** *In situ* PXRD patterns of CO<sub>2</sub> loaded **SOF-7a** in the pressure range 0 to 1 bar.

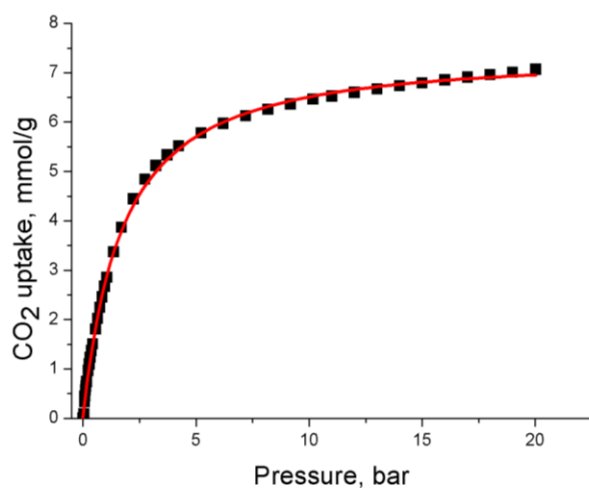


**Figure S9** CO<sub>2</sub> isotherm at 273 K, black squares: experimental data fitted using Tóth model (red line).

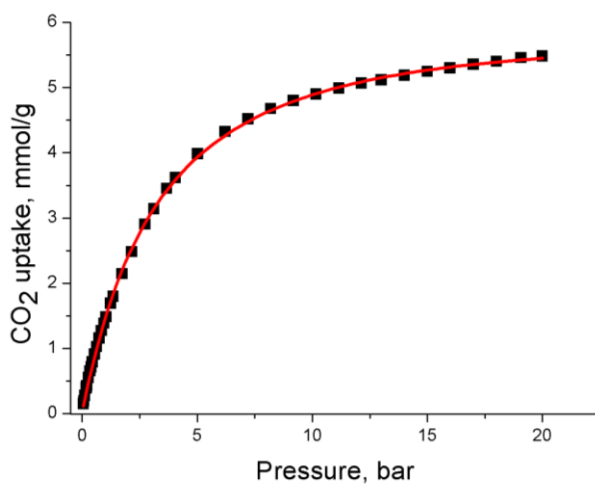


**Figure S10** CO<sub>2</sub> isotherm at 298 K, black squares: experimental data fitted using Tóth model (red line).



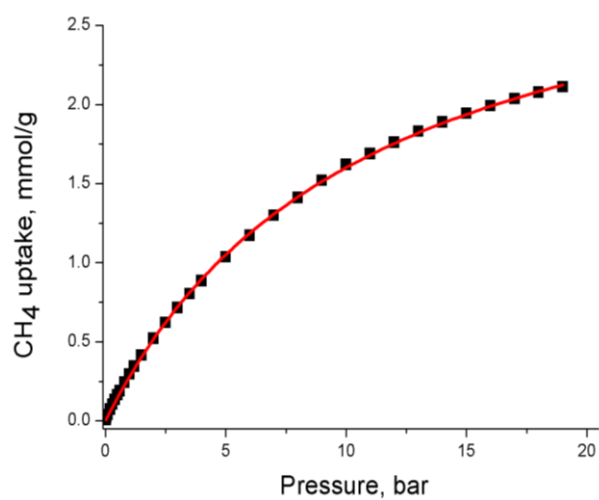


**Figure S11** CH<sub>4</sub> isotherm at 273 K, black squares: experimental data fitted using Tóth model (red line).

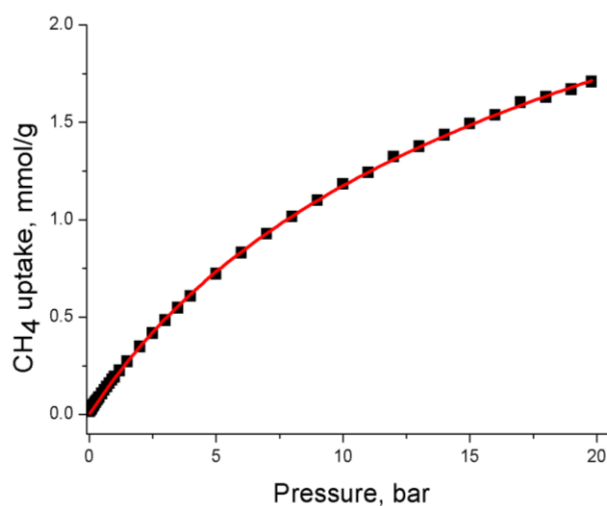


**Figure S12** CH<sub>4</sub> isotherm at 298 K, black squares: experimental data fitted using Tóth model (red line).

## References

- [S1] (a) Yang, W.; Greenaway, A.; Lin, X.; Matsuda, R.; Blake, A. J.; Wilson, C.; Lewis, W.; Hubberstey, P.; Kitagawa, S.; Champness, N. R.; Schröder, M. *J. Am. Chem. Soc.* **2010**, *132*, 14457; (b) Ghozlan, S. A. S.; Hassanién, A. Z. A. *Tetrahedron* **2002**, *58*, 9423.
- [S2] Alsmail, N. H.; Suyetin, M.; Yan, Y.; Cabot, R.; Krap, C. P.; Lü, J.; Easun, T. L.; Bichoutskaia, E.; Lewis, W.; A. Blake, J.; Schröder, M. *Chem. Eur. J.* **2014**, *20*, 7317.
- [S3] Sheldrick, G. M. SHELXS97. *Acta Crystallogr., Sect. A* **2008**, *64*, 112.
- [S4] Spek, A. L. *Acta Crystallogr., Sect. D* **2009**, *65*, 148.
- [S5] Potoff, J. J.; Siepmann, J. I. *AIChE J.* **2002**, *47*, 1676.
- [S6] Jorgensen, W. L.; Maxwell, D. S.; Tirado-Rives, J. *J. Am. Chem. Soc.* **1996**, *118*, 11225.
- [S7] Yang, Q.; Zhong, C. *J. Phys. Chem. B* **2006**, *110*, 17776.
- [S8] Peng, D.-Y.; Robinson, D. B. *Ind. Eng. Chem. Fundam.* **1976**, *15*, 59.
- [S9] Shao, Y. et al. *Phys. Chem. Chem. Phys.*, 2006, *8*, 3172.
- [S10] Gupta, A.; Chempath, S.; Sanborn, M. J.; Clark, L. A.; Snurr, R. Q. *Mol. Simul.* **2003**, *29*, 29.
- [S11] Grimme, J.; Antony, S.; Ehrlich, H.; Krieg, J. *Chem. Phys.* **2010**, *132*, 154104.
- [S12] Luo, X.-Z.; Jia, X.-J.; Deng, J.-H.; Zhong, D.-C. *J. Am. Chem. Soc.* **2013**, *135*, 11684.
- [S13] Mastalerz, M.; Opperl, I. M. *Angew. Chem. Int. Ed.* **2012**, *51*, 5252.
- [S14] He, Y.; Xiang, S.; Chen, B. *J. Am. Chem. Soc.* **2011**, *133*, 14570.
- [S15] Li, P.; He, Y.; Guang, J.; Weng, L.; Zhao, J. C.-G.; Xiang, S.; Chen, B. *J. Am. Chem. Soc.* **2014**, *136*, 547.
- [S16] (a) Thallapally, P. K.; McGrail, B. P.; Atwood, J. L.; Gaeta, C.; Tedesco, C.; Neri, P. *Chem. Mater.* **2007**, *19*, 3355; (b) Msayib, K. J.; Book, D.; Budd, P. M.; Chaukura, N.; Harris, K. D. M.; Helliwell, M.; Tedds, S.; Walton, A.; Warren, J. E.; Xu, M.; McKeown, N. B. *Angew. Chem., Int. Ed.* **2009**, *48*, 3273.
- [S17] (a) Sozzani, P.; Bracco, S.; Comotti, A.; Ferretti, L.; Simonutti, R. *Angew. Chem. Int. Ed.* **2005**,

44, 1816 ; (b) Couderc, G.; Hertzsch, T.; Behrnd, N.-R.; Krämer, K.; Hulliger, J. *Microporous Mesoporous Mater.* **2006**, 88, 170.

[S18] Kim, H.; Kim, Y.; Yoon, M.; Lim, S.; Park, M. S.; Seo, G.; Kim, K. *J. Am. Chem. Soc.* **2010**, 132, 12200.

[S19] Tian, J.; Ma, S.; Thallapally, P. K.; Fowler, D.; McGraila, B. P.; Atwood, J. L. *Chem. Commun.* **2011**, 47, 7626.